GPPS | JOURNAL

JOURNAL OF THE GLOBAL POWER AND PROPULSION SOCIETY
journal.gpps.global

# Numerical simulation of effect of blade end slot on performance of compressor cascade

**Original article**

Article history:
**Submission date:** 14 November 2024
**Acceptance date:** 18 May 2025
**Publication date:** 9 December 2025

*Correspondence:
XL: xs-li@mail.tsinghua.edu.cn

Peer review:
Single blind



Keywords:
blade end slot; compressor cascade test; profile performance; corner separation control

Citation:
Wang Z., Li X., Ren X., and Gu C. (2025). Numerical simulation of effect of blade end slot on performance of compressor cascade. Journal of the Global Power and Propulsion Society. 9: 318–329.
https://doi.org/10.33737/jgpps/205267

Ziyuan Wang[1], Xuesong Li[1,*], Xiaodong Ren[1], Chunwei Gu[1]

[1]*Department of Energy and Power Engineering, Tsinghua University, 30 Shuangqing Road, Haidian District, Beijing 100084, P.R. China*

## Abstract

Flow in test of highly loaded compressor cascade often deviates from the two-dimensional flow due to end-wall separation. As a traditional method, boundary layer suction often has problems, such as complicated device and unclear required suction flow rate. In this work, a novel method for cascade tests, blade end slot, was proposed to make test results better reflect the performance of two-dimensional profile in a highly loaded compressor cascade. The effect of slot jet flow on end-wall separation was investigated. The results show that slots can effectively suppress corner separation and make the flow at mid-span tend to two-dimensional flow. The slot jet flow near the core of corner separation can speed up the low-energy fluid in the corner region and suppress the separation. When the slot is of 10% span height and at about 80% chordwise position, the performance deviation between mid-span of cascade and the two-dimensional profile is less than 5% at large positive incidence positions.

## Introduction

Cascade test is an important means to obtain compressor profile performance. A large number of cascade tests have been carried out to study the performance of classical two-dimensional profiles . Due to the limited spanwise size of the test cascade, flow separation will occur at the end-wall, resulting in blockage of the end-wall flow and contraction of the main flow path. Axial velocity density ratio (AVDR) will be large, and flow in mid-span will deviate from the two-dimensional flow. To make the test results accurate and reliable, it is necessary to control the end-wall separation to reduce the AVDR.

End-wall suction and blade slotting are the methods that can be used to control separation. End-wall suction is an active control method that reduces separation by directly suck out low-energy fluid near the end-wall. Many studies have adopted end-wall suction in cascade test (Erwin and Emery, 1951; Herrig et al., 1957; Song and Ng, 2004; Starken et al., 1975), and achieved good results. However, end-wall suction requires additional equipment and energy. On the other hand, for different cascades and working conditions, the size and position of the end-wall separation are different, and the required extraction volume and position are also different. The corresponding guidelines are lacking.

Blade slotting is a passive control method. By opening a channel between the pressure surface and the suction surface of the blade, the fluid flows from the pressure surface to the suction surface along the channel driven by the pressure difference, which forms a jet impact on the low-energy fluid and weakens the separation. The concept of blade

slotting was first introduced into compressor by Rockenbach (1968), and a series of experimental studies were conducted by NASA (Keenan and Bartok, 1968; Mikolajczak et al., 1970; Rockenbach, 1968). They made slots in different rotors and stators and compared them with datum blades. The results show that blade slotting can control the trailing edge separation and reduce the wake width, but it cannot control the separation near the end-wall. The scholars have carried out slot research on the cascades. Zhou et al. (2008a,b, 2010) conducted full-span slotting and studied the effects of different slot widths, angles and positions on cascade performance through experimental and numerical methods. Ramzi et al. (2011), Ramzi and Abderrahmane (2013) conducted numerical calculations of slot on 2D profile and full-span slot on 3D cascade, and believed that slotting could control the suction surface separation and end-wall separation. Wang et al. (2012) found that when the negative incidence angle is large, the slotted cascade may increase the suction surface separation, which makes the cascade performance worse. Jiaguo et al. (2018) developed a slotted control method for high-load cascade separation, and conducted experimental and numerical studies. It is found that jet inhibits the development of corner separation. Blade slotting greatly improves the aerodynamic performance of the cascade under separation conditions, but causes additional losses without separation conditions. Because the full span of cascade is slotted, the 2D profile is actually changed.

Blade end slotting has also been studied by scholars. Compared with full-span slot, end slot can control the separation of corner regions without changing the two-dimensional profile at mid-span. Tang et al. (2019, 2020) compared the full-span slot and the end slot (20% span) in a cascade, and found that both the full-span slot and the end-slot could change the flow structure near the end-wall and recombine the flow at a large positive incidence angle. The adaptive jet of the channel charges the low momentum fluid downstream, inhibits its migration to mid-span, thus reducing the corner separation and improving the performance. However, the loss of the full-span slotted cascade may be larger than that of the end-slotted cascade due to the mixing of the jet and the main flow at mid-span. Liu et al. (2016) studied the effect of end slot of different solidity and aspect ratio. Sun et al. (2021) optimized the shape of the slot. Ma et al. (2021) studied the influence of blade end slots on corner separation caused by shock wave/boundary layer interaction for a supersonic compressor cascade, and compared four different blade end slots. It was found that the blade end slot improved the corner separation, and the optimal position was slightly downstream of the initial separation point. For the compressor stage, Yoon et al. (2019) conducted end slot for a three-stage compressor and found that the slotting enhanced the axial momentum near hub while weakened the radial migration, thus weakening the corner separation near hub.

The previous research mainly analyses and optimizes cascade slotting for the purpose of weakening separation and improving cascade performance. For the cascade test to obtain performance of two-dimensional profile, the purpose of control separation is to reduce the influence of end-wall separation on the mid-span flow and restore the two-dimensional flow at mid-span. It is not important to reduce the end zone loss and enlarge the diffusion factor of cascade. How to achieve the above purpose through blade slotting still needs to be studied.

This paper proposes a method of blade end slot for cascade test. The slotting controls the end-wall separation and helps the flow at mid-span to become two-dimensional. Firstly, cascade and slot geometry are introduced. Then the numerical method is introduced. Thirdly, the effect of blade end slot on the performance at mid-span is compared, and flow at mid-span is analysed. Next, 3D flow structures are exhibited and the effect of slot jet on corner separation is analysed. Finally, main conclusions are illustrated.

## Geometric model

### High load compressor cascade

The datum profile investigated in this work is cut-off at the mid-span of a certain axial compressor rotor. Limited by the test facility, chord length was scaled down to 0.5 times for a higher aspect ratio. Table 1 lists the design parameters for the profile after scaling. Cascade tests were performed on a variable density plane cascade wind tunnel at China Aerodynamics Research and Development Center (CARDC). Detailed test introduction, including test facilities parameters, measurement methods, test conditions, etc., and test results have been published by Wang et al. (2024).

### Slot design

In order to introduce a suitable jet flow near the end-wall to control the corner separation, the slot design was carried out. The design parameters of slot are presented in Figure 1. The aim of slotting is to control the flow in the mid-span of the cascades to be close to two-dimensional flow so as to reflect the real performance of profiles

Table 1. Geometry parameters of the datum profile.

| Parameters | Values | Units |
|---|---|---|
| Chord length | 87.9 | mm |
| Solidity | 2.11 | – |
| Aspect ratio | 2.16 | – |
| Inlet angle | 48.0 | deg |
| Stagger angle | 35.2 | deg |
| Reynolds number | $1.14 \times 10^6$ | – |
| Mach number | 0.6 | – |

in the test, not to improve the performance of the cascade. Therefore, a complex geometry of slots is not necessary, although it may have a good effect in reducing the loss of cascades. Straight slots were chosen because they have the advantage of simple structure and few parameters while satisfying the aim. A blade end slot (covering 10% of the span from the end-wall) was selected to control the separation near the end-wall without affecting the performance of the mid-span of the cascade. Some literatures (Ma et al., 2021; Ramzi et al., 2011; Rockenbach, 1968) suggested that slot should be near the separation start point. However, it mainly reduces the trailing edge separation of the 2D blade, and the effect on the end-wall separation was not obvious (Ramzi and AbdErrahmane, 2013; Rockenbach, 1968). In order for the slot jet flow to impact the center of separation, the outlet of the slot was set at 80% chordwise position. The width of the slot was set to 1.1% of the chord length, and the angle from the axis was 48.8 deg.

## Numerical modeling

### CFD modelling

ANSYS CFX was used in this study to solve the Navier-Stokes equation. Quasi-2D profile, 3D datum cascade and 3D slotted cascades were calculated. The single-passage is adopted due to the periodicity of the cascade. Half of blade passage in the spanwise direction was considered because the flow in cascade symmetrically along the plane of 50% span. Extension sections with 1- and 2-times chord length were arranged upstream and

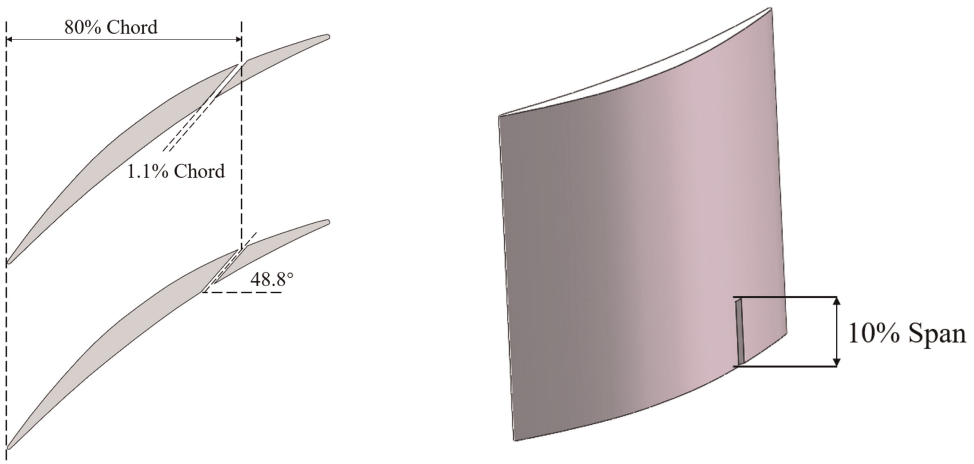


Figure 1. Slot configuration.

downstream of the cascade. The measuring position of the inlet and outlet flow was 50% chord length away from the leading and trailing edge, which is the same as the measurements in test.

The total pressure and static temperature at the inlet boundary and the static pressure at the outlet boundary measured in the test were set in the simulation, which ensured that the inlet Mach number was consistent with the test value. No-slip and adiabatic conditions were imposed on all solid walls, including surface of blade and slot and end-wall. For 3D simulation, 50% span section was set to symmetric plane. For the quasi-2D calculation, the upper and lower end-walls were set as periodic boundaries, and the flow of the two-dimensional profile was simulated by an infinite cascade. The SST turbulence model was used to account for the turbulence flow. The free stream turbulence intensity was set as $Tu = 1\%$ at the inlet according to test.

## Mesh

The meshes for the simulation were generated using the NUMECA Autogrid5. Figure 2 shows the meshes for datum cascade and 3D slotted cascades. The structured multi-block O4H grid was used for the datum blade. For quasi-2D and 3D datum cascades, a series of grids with different densities and distributions were compared with guarantee grid independence. The final grid for the datum blade has 2.3 million grid points with 77 nodes in the spanwise direction. A H-block grids was added for the slot on the basis of the datum blade mesh. About 0.12 million grid points were chosen, which satisfies grid independence. The meshes were added to the main flow passage to ensure the one-to-one correspondence of the mesh nodes at the junction and optimize the local mesh expansion ratio (mainly for the boundary layer mesh in slot). The final grid for the slotted blade has 3.8 million grid points. The $y^+$ calculated was less than 1 for all simulations.

## Validation of simulations

Comparisons were made between test results and simulation results. The total pressure loss coefficient $\omega$, defined by Equation (1), was compared in Figure 3. In Equation (1), $\overline{P}_{t,2}$ means outlet total pressure, $\overline{P}_{t,1}$ means inlet total pressure and $\overline{P}_{s,1}$ means inlet static pressure, which are all massflow-average results.

$$\omega = \frac{\overline{P}_{t,2} - \overline{P}_{t,1}}{\overline{P}_{t,1} - \overline{P}_{s,1}}. \tag{1}$$

Within positive and negative stall boundaries (twice the minimum loss conditions) except for the incidence angle of −3 deg, the deviations of total pressure loss $\omega$ between simulation and test results are less than 5%. When incidence angle is −3 deg, there is a shock in the passage due to the large negative incidence angle, shown in Figure 4. Static pressure coefficient distribution $C_p$, defined by Equation (2), on the blade surface at the mid-span of the simulation and tests were also shown in Figure 3. In Equation (2), $P_s$ means local static pressure. $\overline{P}_{s,1}$ means inlet static pressure and $\overline{P}_{t,1}$ means inlet total pressure, which are both massflow-average results.

$$C_p = \frac{P_s - \overline{P}_{s,1}}{\overline{P}_{t,1} - \overline{P}_{s,1}}. \tag{2}$$

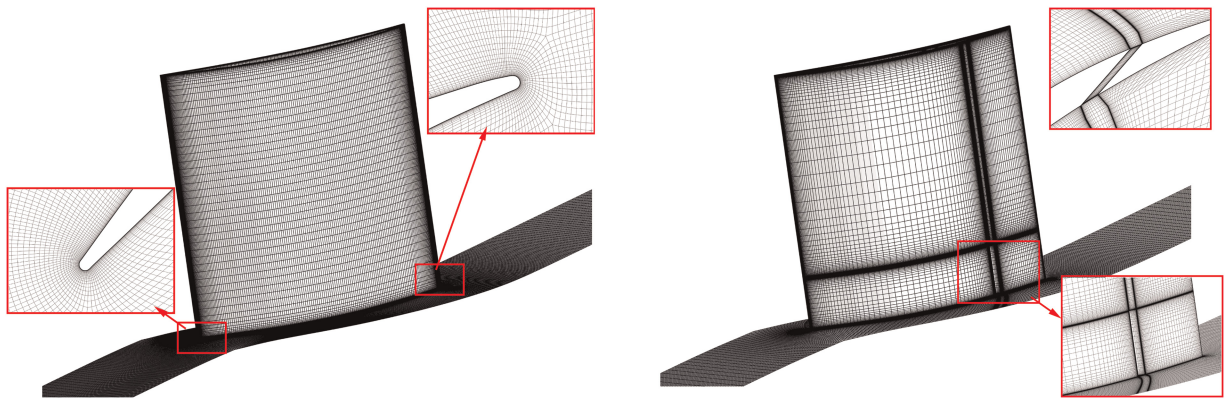

Figure 2. Meshes of datum cascade (left) and slotted cascade (right).

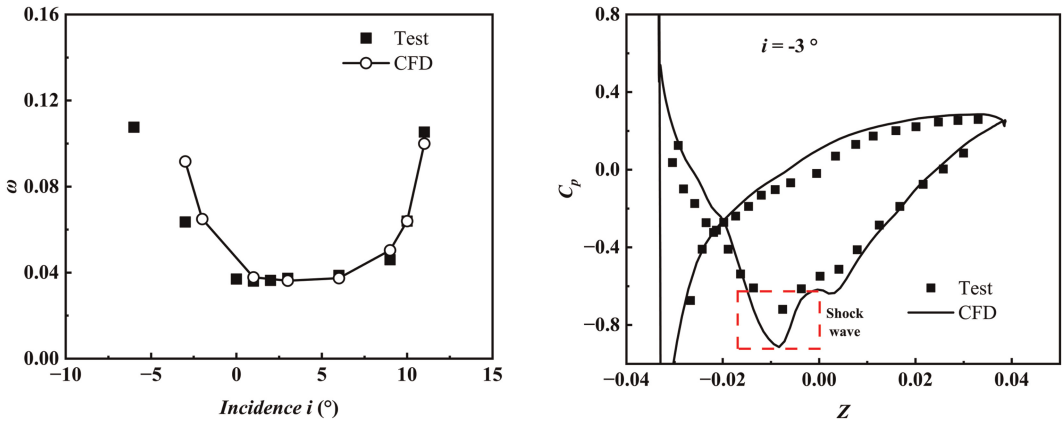


Figure 3. Comparison of total pressure loss coefficients (left) and static pressure coefficients (right) between test and CFD of datum cascade.

The intensity of the shock wave in the simulation result is greater than the test results. The difference in the loss when incidence angle is −3 deg was mainly produced in the shock wave. The streamlines on blade surface of test and simulation were also compared in Figure 5. The simulation of different incedences can well predict the region of separation. Based on the above comparison, simulations in this paper are reliable.

## Results and discussions

### Mid-span performance

For cascade test, the performance at mid-span was of interest. In order to obtain the performance of the 2D profile in test, the flow and performance at mid-span of cascade should be closer to the 2D results. Figure 6 shows the total pressure loss $\omega$ and deviation angle $\delta$ for 2D profile, and mid-span of 3D datum and slotted cascade. It can be seen that there is a large deviation in the prediction of the total pressure loss $\omega$ of the 2D profile by the 3D prototype cascade. When $i = +1°$ (minimum loss condition), the relative deviation between results of the 3D datum cascade and the 2D profile is 1.08%. When $i = -3°$ (negative incidence condition), the relative deviation between the two is 26.39%. When $i = +9°$ (positive incidence condition), the relative between the two is 22.27%. The same goes for deviation angle $\delta$. At different incidences, the predicted errors of deviation angle $\delta$ of 3D datum cascade for the 2D profile results are around 1.5–2 degrees. The performance difference shows that for this profile, the test results of the 3D datum cascade are difficult to accurately predict the

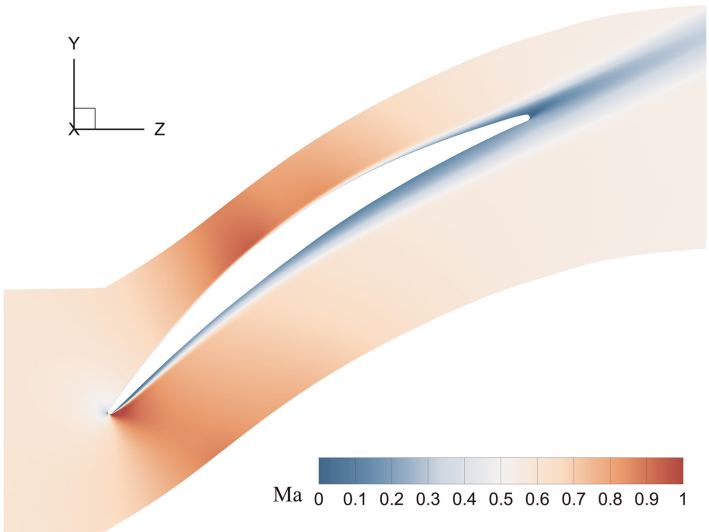


Figure 4. Mach number contour at 50% span of CFD result when incidence is −3 deg.

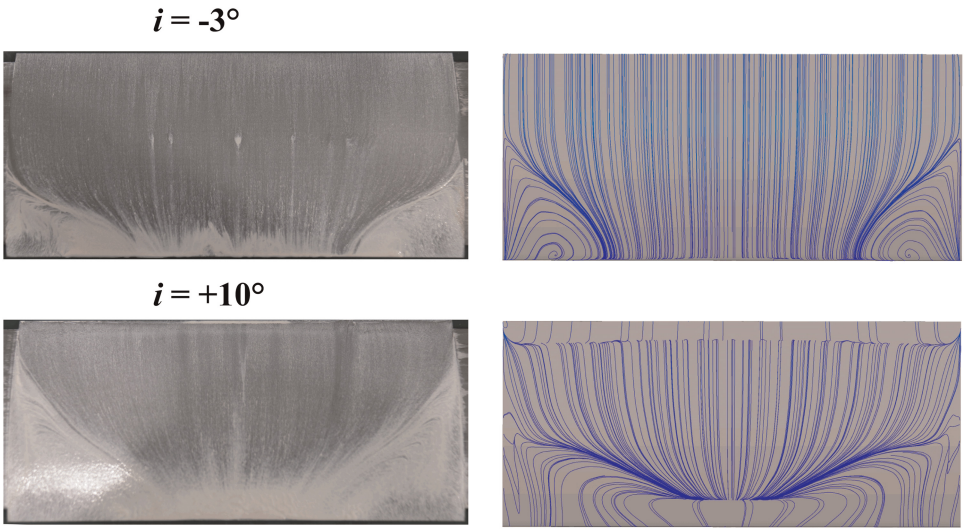


Figure 5. Streamlines of test and CFD of datum cascade.

performance of profile due to the influence of end-wall separation. Especially in the positive incidence conditions, which are more dangerous conditions, the results of the 3D datum cascade may underestimate the loss of the profile, making the expectations too optimistic, thus affecting the blade design.

The slotted cascade better predicts the performance of the 2D profile compared to the datum cascade. When $i = +1°$, the predicted total pressure loss $\omega$ of the slotted cascade is basically consistent with that of the datum cascade. When $i = -3°$, the relative deviation of the calculated total pressure loss $\omega$ between slotted cascade and 2D profile is reduced to 7.28%. When $i = +9°$, the relative deviation between the two is reduced to 4.48%. The situation where losses may be underestimated under positive incidence conditions has been improved. The maximum deviation angle $\delta$ is also reduced to 0.7 deg, among which the errors at the minimum loss condition and the positive incidence condition are both less than 0.5 deg. In the entire range of incidence angles, the test results using 3D slotted cascades can better obtain the performance of this profile.

Figure 6 also shows the changes in AVDR under different incidence angles. AVDR is defined by Equation (3), in which $\overline{\rho}_1$ and $\overline{\rho}_2$ means inlet and out density, $\overline{V}_{z,1}$ means inlet and outlet axial velocity, which are both massflow-average results. The larger AVDR of the three-dimensional cascade, the stronger influence of the three-dimensional flow, and the stronger the end-wall blockage on the flow passage in the blade. AVDR of the two-dimensional blade is 1. The results show that the AVDR of the datum cascade is above 1.1 and increases with the increase of the incidence. AVDR of slotted blades is all reduced, which is around 1.05, except for the large negative incidences. The flow in the slotted cascade is closer to two-dimensional flow.

$$\mathrm{AVDR} = \frac{\overline{\rho}_2 \cdot \overline{V}_{z,2}}{\overline{\rho}_1 \cdot \overline{V}_{z,1}}. \tag{3}$$

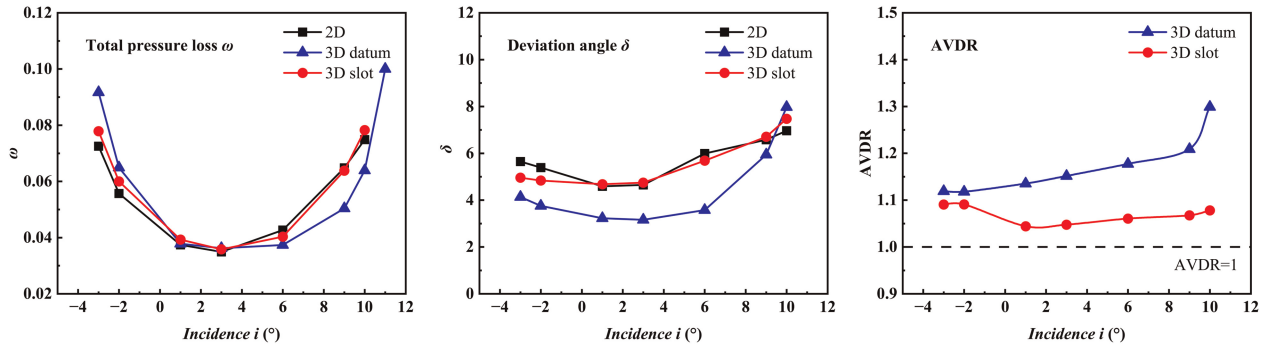


Figure 6. Performance varying with incidence at mid-span (left: total pressure loss, middle: deviation angle, right: AVDR).

Streamlines and Mach number contours at mid-span at typical incidence angles are compared in Figure 7, to analyse the effect of slotting on the flow in the cascade. The results show that the flow of the slotted blade in the blade is closer to the 2D profile flow. When $i = +9°$, due to large positive incidence angle, the two-dimensional profile flow has a large trailing edge separation on suction surface. In the 3D datum cascade, the trailing edge separation is significantly reduced. This is because the AVDR of the 3D datum cascade is large, the flow channel in the blade is compressed, the flow is accelerated, and the trailing edge separation on the suction surface is suppressed. After blade slotting, the AVDR decreases, the flow acceleration in the blade weakens, and the trailing edge separation on the suction surface returns to the state of the 2D profile flow. The increase in separation causes the high total pressure loss and deviation angle at mid-span, which return to the level of the 2D profile. When $i = +1°$, the flow changes caused by slotting are similar to those of $i = +9°$. However, since the trailing edge separation on suction surface of the 2D profile flow is small when $i = +1°$, the flow changes among the three are very small, and the overall performance is basically unchanged. When $i = -3°$, a compression wave appears in the 2D profile channel. The flow acceleration caused by AVDR leads to enhanced compression waves and increased loss. After slotting, the AVDR is reduced, the compression wave intensity is reduced, and the loss is reduced.

Comprehensively, blade end slot on cascade reduces the AVDR, restores the flow in cascade to 2D flow, and better predicts the performance of the 2D profile.

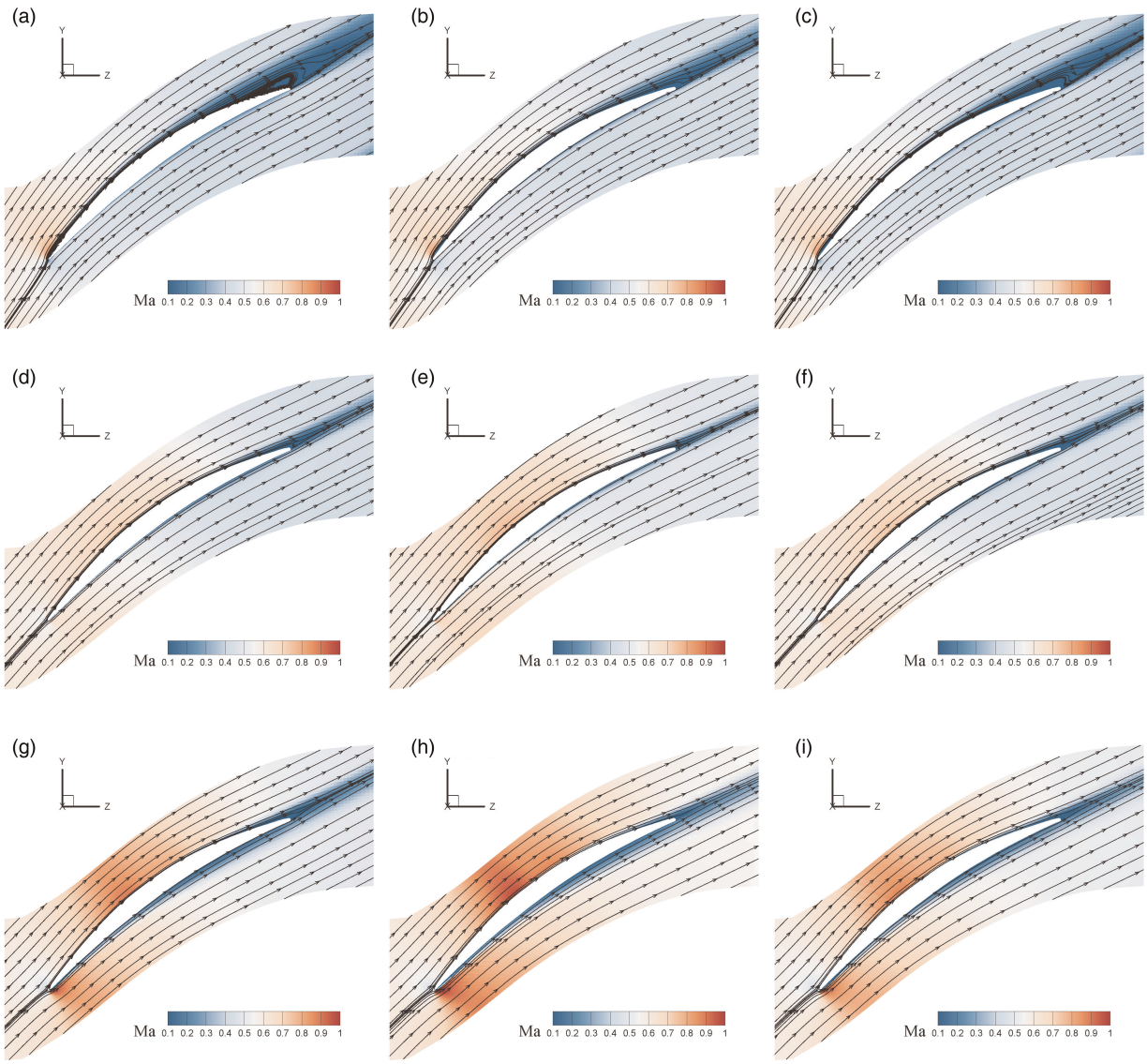


Figure 7. Mach number contours and Streamlines under typical incidences: (a) 2D, +9 deg, (b) datum, +9 deg, (c) slot, +9 deg, (d) 2D, +1 deg, (e) datum, +1 deg, (f) slot, +1 deg, (g) 2D, −3 deg, (h) datum, −3 deg, (i) slot, −3 deg.

## 3D flow structures

The three-dimensional flow structure of datum cascade and slotted cascade when $i = +9°$ are exhibited, and the effect of blade end slots is analysed entropy contours and streamlines for 5% span is shown in Figure 8. Separation and the slot jet can be observed. A large separation occurs near the trailing edge on the suction surface of the datum cascade. In the slotted cascade, driven by the pressure difference from the pressure surface to the suction surface, the slot jet rushes into the separation zone on the suction surface along the slot direction and flows downstream of the blade along the suction surface. The high-energy fluid of the jet accelerates the low-energy fluid in the separation. The higher axial momentum slot jet carries drive the backflow near the trailing edge to flow downstream of the blade and clears the flow passage. The jet "disperses" the corner separation near suction surface and reduces end-wall blockage.

Figure 9 shows the pressure gradient contours and streamlines on the blade and end wall surfaces, reflecting the flow and separation on the wall. The pressure gradient in the blade height direction (X direction), $dp/dx$, is contoured on the blade surface, and the pressure gradient in the circumferential direction (Y direction), $dp/dy$, on the end-wall. Red indicates a positive pressure gradient and blue indicates a negative pressure gradient.

Corner separation occurs in the corner near the suction surface of the datum cascade. Driven by the positive pressure gradient in Y direction on the end-wall near the trailing edge, the end-wall boundary layer mixes with the trailing edge separation, forming a backflow near the end-wall at outlet and blocking the flow. The blockage causes a large negative pressure gradient in X direction on the front blade surface, pushing the incoming flow upstream to move toward the mid-span starting from the position about 40% of the chord. Finally, the flow channel at mid-span is squeezed.

The slot jet of the slotted cascade changes the three-dimensional flow in the corner. The jet changes the positive pressure gradient in Y direction at the end-wall, pushing the low-energy fluid away from the blade surface and relieving the blockage of the slot outlet and its downstream. The newly formed separation upstream of the slot outlet is suppressed by the jet, failed to form a large separation. The separation in the corner zone is suppressed, which reduces the blockage in the end-wall. The upstream flow is driven by less pressure difference toward the mid-span, and the flow is squeezed less. Since the flow is not significantly accelerated, a large trailing edge separation reappears at mid-span, which is the flow phenomenon that should appear in two-dimensional flow of this profile.

Vorticity magnitude contours and 3D streamlines for different S3 stream surfaces are shown in Figure 10, and the development of vortices in the blade passage can be observed. In the datum cascade, the suction surface leg of horseshoe vortex begins to move upward at position about 40% of the chord, and is drawn into the trailing edge separation. The end-wall boundary layer is involved in the separation and flows back downstream of the trailing edge, aggravating the blockage. The low-energy fluid in the corner area continues to accumulate, forming corner separation covering ranges about 35% span. In the slotted cascade, upstream of the slot outlet, the horseshoe vortex also moves upward to form a local vortex. However, it is pushed away from the blade surface under the impact of the slot jet, and then flows downstream along the mainstream direction after being accelerated. Near 10% span, that is, at the upper end of the slot, the slot jet flow is small. It separates and mixes with the

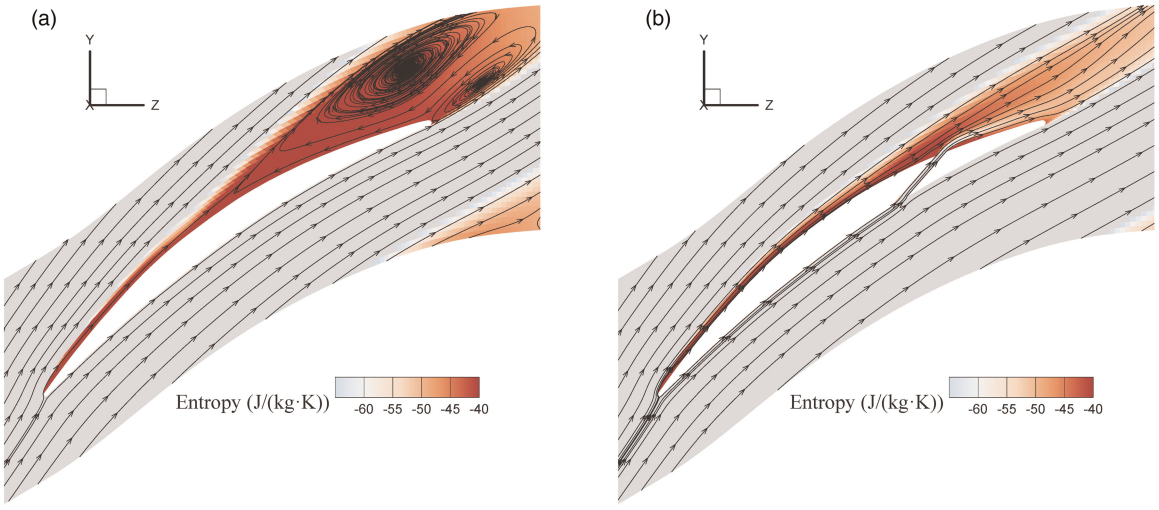


Figure 8. Entropy contours and Streamlines at 5% span when incidence is +9 deg (a) datum, (b) slot.

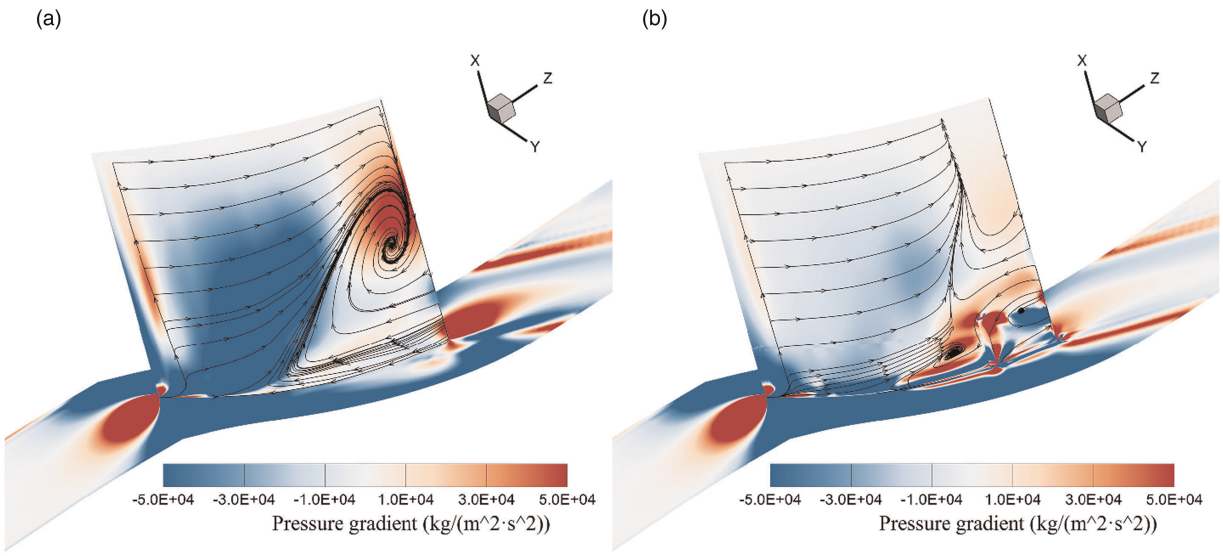


Figure 9. Pressure gradient contours and Streamlines on blade surface and end-wall when incidence is +9 deg (a) datum, (b) slot.

trailing edge boundary layer to form a new separation. Since this separation is caused by the disturbance of the slot jet to the trailing edge separation, the separation range is small and the location is close to the downstream, so it has little impact on the flow above 20% span.

The yaw angle is resolved by the arc tangent ratio of the circumferential velocity to the streamwise velocity.

$$\beta = \arctan\left(\frac{V_y}{V_z}\right). \tag{4}$$

Figure 11 shows the yaw angle contours of the S3 stream surface at 20% chord downstream of the trailing edge. In the corner area of the datum cascade, a recirculation zone covering about 15% span appears, and a narrow trailing edge separation occurs above 20% span. In the corner area of the slotted cascade, the original separation area disappears and two new separations appear. The passage vortex formed between the suction surface leg of horseshoe vortex and the end wall boundary layer near the end wall (below 5% span). Due to the push of the slot jet, the passage vortex fails to mix with the trailing edge separation and fails to develop upward along the blade surface. The slot jet and trailing edge boundary layer form a vortex at about 10% span. The two

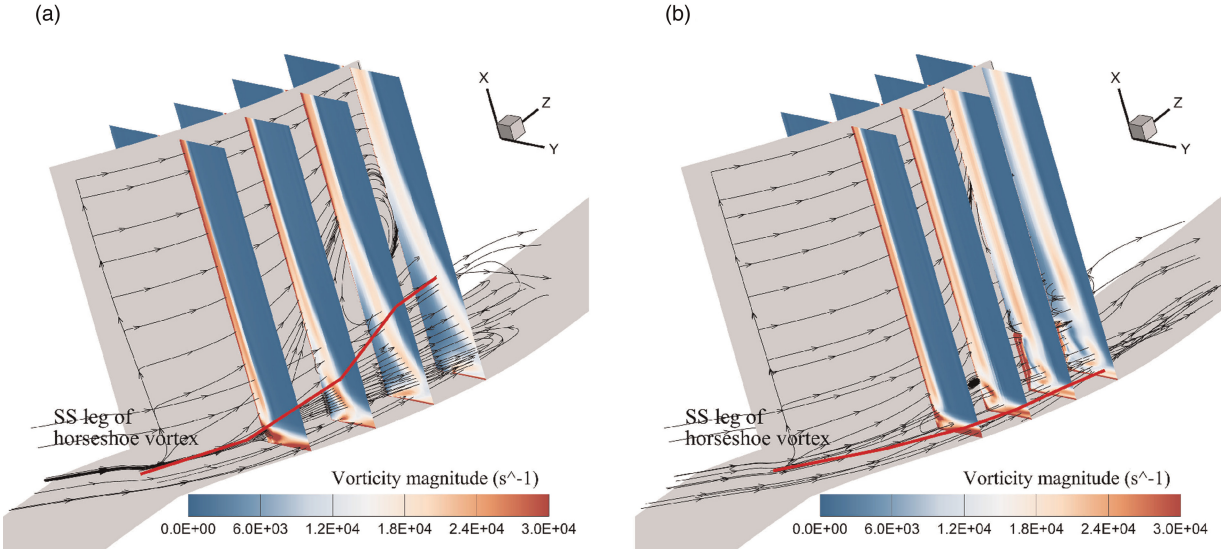


Figure 10. Vorticity magnitude contours on S3 stream surfaces and 3D Streamlines when incidence is +9 deg (a) datum, (b) slot.

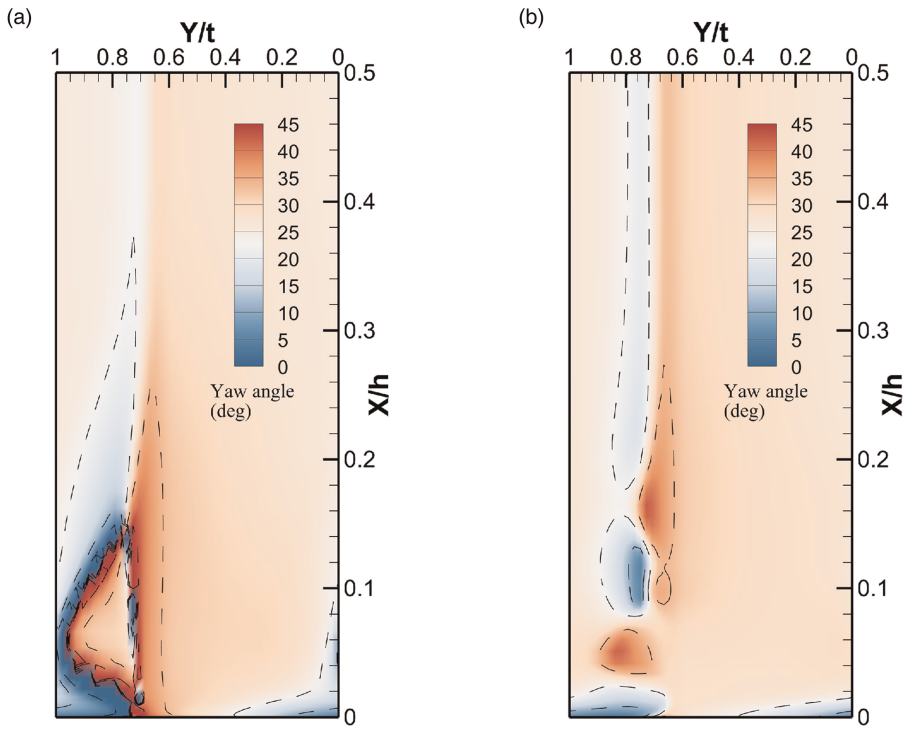


Figure 11. Yaw angle distribution on S3 stream surface (20%c downstream the TE) when incidence is +9 deg (a) datum, (b) slot.

separations failed to mix and develop under the splitting of the slot jet. Above 20% span, a wide trailing edge separation appears, which is the trailing edge separation of the 2D profile at this incidence ($i = +9°$).

## Conclusions

In this work, a novel method for cascade tests, blade end slot, was proposed to make test results better reflect the performance of two-dimensional profile in a highly loaded compressor cascade. Through the calculation results of 2D and 3D CFD, the performance and three-dimensional flow structures of the 2D profile, 3D datum cascade and slotted cascade were compared and analysed. The results show that blade end slot is a feasible test method. Conclusions are as follows:

1. Blade end slot reduces the AVDR of the cascade and weakens the flow acceleration in the mid-span. The trailing edge separation at mid-span of the cascade increases under positive incidence angle and the compression wave weakens under negative incidence angle, which is closer to the flow of a two-dimensional profile. The slot designed in this work covers 10% span near the end-wall and the slot outlet is at position of 80% chord. This solution reduces the deviation of performance between 3D cascade and 2D profile. In positive incidence conditions, which are more dangerous to operation, the relative deviations of total pressure loss are less than 5%, and the errors of deviation angle are less than 0.5°.
2. The slot jet brought by the slotted cascade controls the corner separation and reduces blockage near the end-wall. The jet pushes the suction surface leg of horseshoe vortex and the end-wall boundary layer away from the blade surface, hindering further development of separation. At the same time, the jet accelerates the low-energy fluid near the trailing edge at the end wall to flow downstream, preventing the fluid from forming a backflow in the corner area. Two new separation zones are formed at the outlet of the cascade, the separation area and blockage are smaller than the corner separation of the datum cascade.

## Funding sources

This work was supported by the National Science and Technology Major Project of China (J2019-II-0005-0025).

## Competing interests

Ziyuan Wang declares that he has no conflict of interest. Xuesong Li declares that he has no conflict of interest. XIaodong Ren declares that he has no conflict of interest. Chunwen Gu declares that he has no conflict of interest.

# Nomenclature

## Symbols

### English Symbols

| | |
|---|---|
| $C$ | Chord length |
| $C_p$ | Static pressure coefficient |
| $I$ | Incidence angle (deg) |
| Ma | Mach number |
| $P$ | Pressure (Pa) |
| Re | Reynolds number |
| $T$ | Temperature (K) |
| $Tu$ | Free stream turbulence intensity |
| $V$ | Velocity (m/s) |

## Greek Symbols

| | |
|---|---|
| $\beta$ | yaw angle (deg) |
| $\delta$ | Deviation angle (deg) |
| $\rho$ | Density (kg/m$^3$) |
| $\sigma$ | Blade pitch |
| $\omega$ | Total pressure loss coefficient |

## Abbreviations

| | |
|---|---|
| 2D | Two-dimensional |
| 3D | Three-dimensional |
| AVDR | Axial velocity density ratio |
| CFD | Computational fluid dynamics |

## Subscripts

| | |
|---|---|
| 1 | Inlet |
| 2 | Outlet |
| $S$ | Static parameter |
| $T$ | Total parameter |
| $Y$ | Y direction |
| $Z$ | Z direction |

# References

Erwin J. R. and Emery J. C. (1951). *Effect of tunnel configuration and testing technique on cascade performance*. Washington: Langley Aeronautical Laboratory.

Herrig L. J., Emery, J. C. and Erwin, J. R. (1957). *Systematic two-dimensional cascade tests of NACA 65-series compressor blades at low speeds*. Washington: National Advisory Committee for Aeronautics.

Jiaguo H., Ruren, W., Renkang, L., Chen, H. and Qiushi, L. (2018). Experimental investigation on separation control by slot jet in highly loaded compressor cascade. *Proceedings of the Institution of Mechanical Engineers, Part G: Journal of Aerospace Engineering*. 232 (9): 1704–1714. https://doi.org/10.1177/0954410017703145.

Keenan M. J. and Bartok J. A. (1968). *Experimental evaluation of transonic stators –data and performance report multiple-circular-arc stator a (sllotted)*. NASA CR-54624.

Liu Y., Sun, J., Tang, Y. and Lu, L. (2016). Effect of slot at blade root on compressor cascade performance under different aerodynamic parameters. *Applied Sciences*. 6 (12): 421. https://doi.org/10.3390/app6120421.

Ma J., Yang, G., Zhou, L., Ji, L. and Zhang, C. (2021). Effect of a blade end slot on supersonic compressor cascade hub-corner separation. *Aerospace Science and Technology*. 118: 107032. https://doi.org/10.1016/j.ast.2021.107032.

Mikolajczak A. A., Weingold, H. D. and Nikkanen, J. P. (1970). Flow through cascades of slotted compressor blades. *Journal of Engineering for Power*. 92 (1): 57–64. https://doi.org/10.1115/1.3445300.

Ramzi M. and Abderrahmane G. (2013). Passive control via slotted blading in a compressor cascade at stall condition. *Journal of Applied Fluid Mechanics*. 6 (4): 571–580.

Ramzi M., Bois, G., Eacute, Rard and Abderrahmane, G. (2011). Numerical study of passive control with slotted blading in highly loaded compressor cascade at low mach number. *International Journal of Fluid Machinery and Systems*. 4 (1): 97–103. https://doi.org/10.5293/IJFMS.2011.4.1.097.

Rockenbach R. W. (1968). *Single stage experimental evaluation of slotted rotor and stator blading Part IX - Final Report*. NASA CR-54553.

Song B. and Ng W. (2004). Influence of axial velocity density ratio in cascade testing of supercritical compressor blades. In: *40th AIAA/ASME/SAE/ASEE Joint Propulsion Conference and Exhibit*.

Starken H., Breugelmans, F. A. E. and Schimming, P. (1975). Investigation of the axial velocity density ratio in a high turning cascade. In: *ASME 1975 International Gas Turbine Conference and Products Show*. Vol. Volume 1A: General.

Sun J., Ottavy, X., Liu, Y. and Lu, l. (2021). Corner separation control by optimizing blade end slots in a linear compressor cascade. *Aerospace Science and Technology*. 114: 106737. https://doi.org/10.1016/j.ast.2021.106737.

Tang Y., Liu, Y. and Lu, L. (2019). Evaluation of compressor blading with blade end slots and full-span slots in a highly loaded compressor cascade. *Journal of Turbomachinery*. 141 (12): 121002. https://doi.org/10.1115/1.4044693.

Tang Y., Liu, Y., Lu, L., Lu, H, and Wang, M. (2020). Passive separation control with blade-end slots in a highly loaded compressor cascade. *AIAA Journal*. 58 (1): 85–97. https://doi.org/10.2514/1.J058488.

Wang R., Luo, K., Wu, Y. and Chen, B. (2012). Numerical research on effect of an improved slot configuration on the flow field characteristics of cascade. *Journal of Air Force Engineering University. Natural Science Edition*. 13 (5): 1–4, 19.

Wang Z.-Y., Xiao, Y. B., Li, X. S., Ren, X. D., Gu, C. W., et al. (2024). Experiment and numerical simulation of the performance on scaled compressor cascade and development of a prediction model. *International Journal of Heat and Fluid Flow*. 105: 109243. https://doi.org/10.1016/j.ijheatfluidflow.2023.109243.

Yoon S., Ajay, R., Chaluvadi, V., Michelassi, V. and Mallina, R. (2019). A passive flow control to mitigate the corner separation in an axial compressor by a slotted rotor blade. In: *ASME Turbo Expo 2019: Turbomachinery Technical Conference and Exposition*. Vol. Volume 2A: Turbomachinery.

Zhou M., Wang, R. G., Cao, Z. H. and Zhang, X. Y. (2008a). Research on effect of slot inlet angle and turning angle on the flow field characteristic of cascade. *Journal of Aerospace Power*. 23 (1): 125–129.

Zhou M., Wang, R. G., Zeng, L. j. and Zhao, Y. W. (2008b). Effect of slot width on the aerodynamic performance of compressor cascade. *Journal of Aerospace Power*. 23 (6): 1077–1081.

Zhou M., Zhu, J., Lu, X., Ge, Z., Yan, K. and Huang, R. (2010). Study of flow control using a slotted blade for a compressor airfoil at low reynolds numbers. In: *ASME Turbo Expo 2010: Power for Land, Sea, and Air*. Vol. Volume 7: Turbomachinery, Parts A, B, and C, pp. 279–287.